REPORT DOCUMENTATION PAGE		READ INSTRUCTIONS BEFORE COMPLETING FORM
1. REPORT NUMBER NRL Memorandum 4860	2. GOVT ACCESSION NO. AD - A119569	3. RECIPIENT'S CATALOG NUMBER
4. TITLE *(and Subtitle)* FLASH X RADIOGRAPHY OF LASER-ACCELERATED TARGETS		5. TYPE OF REPORT & PERIOD COVERED A continuing report
		6. PERFORMING ORG. REPORT NUMBER
7. AUTHOR(s) R. R. Whitlock, S. P. Obenschain, and J. Grun*		8. CONTRACT OR GRANT NUMBER(s)
9. PERFORMING ORGANIZATION NAME AND ADDRESS Naval Research Laboratory Washington, DC 20375		10. PROGRAM ELEMENT. PROJECT, TASK AREA & WORK UNIT NUMBERS DE-AI108-79DP40092 AI08-79DP, 40092 (1-72) 47-0859-0-2
11. CONTROLLING OFFICE NAME AND ADDRESS U. S. Department of Energy Washington, DC 20545		12. REPORT DATE August 30, 1982
		13. NUMBER OF PAGES 9
14. MONITORING AGENCY NAME & ADDRESS(*if different from Controlling Office*)		15. SECURITY CLASS. *(of this report)* Unclassified
		15a. DECLASSIFICATION/DOWNGRADING SCHEDULE
16. DISTRIBUTION STATEMENT *(of this Report)* Approved for public release; distribution unlimited.		
17. DISTRIBUTION STATEMENT *(of the abstract entered in Block 20, if different from Report)*		
18. SUPPLEMENTARY NOTES *Mission Research Corporation, Alexandria, VA		

19. KEY WORDS *(Continue on reverse side if necessary and identify by block number)*

Laser-Fusion	Symmetry	Double Foils
Laser-Plasma	X-Ray Backlighting	
Acceleration	Pressure	
Hydrodynamic Efficiency	Smoothing	

20. ABSTRACT *(Continue on reverse side if necessary and identify by block number)*

Flash x radiography of ablatively accelerated planar foils has provided quantitative measurements and qualitative observations regarding several parameters of critical interest to direct illumination laser fusion. A 1.05 micron, 3.3 nsec driver beam was focused onto carbon foils in a large (0.7-1 mm diameter) spot to reduce edge effects. From images produced by a backlighting x-ray flash, we have measured overall coupling efficiency, smoothing of laser nonuniformities, target velocity, and ablation pressure. The high velocity targets maintain a localized, high density (> 3% of solid). In contrast to other workers' recent measurement of pressure from x-ray imaging, our

(Continued)

DD FORM 1473 EDITION OF 1 NOV 65 IS OBSOLETE
1 JAN 73
S/N 0102-014-6601

20. ABSTRACT (Continued)

x-radiographic results, including pressure, are in general agreement with earlier NRL studies. Our results have also provided further insights into double foil interactions and planar target preheat measurements.

FLASH X RADIOGRAPHY OF LASER-ACCELERATED TARGETS*

Direct illumination of spherical pellet shells by laser light in a moderate intensity regime somewhat above 10^{14} W/cm^2 may permit inertial confinement fusion to be achieved.[1] To that end, studies at NRL[2-11] have been directed to the physics of the laser-pellet interaction and of the efficient acceleration of pellet shells to fusion-like velocities.[1] To experimentally model spherical pellets early in the implosion phase, we use planar targets and large focal spots. These experiments have shown that the moderate intensity, direct illumination approach scales favorably in several areas of physics which have been identified as critical elements for laser fusion,[2] and that, therefore, further extention of these experimental studies to a regime closer to reactor conditions is warranted. In the present work, we used a flash x-ray probe to temporally resolve the position of the dense region of accelerated foils; from this, we quantitatively measured the ablation pressure, the target velocity, and the uniformity of target velocity. We also gained further insights into double foil interactions and target preheat measurements.

In earlier work,[7-9] visible probes, operating within limitations imposed by absorption and refraction, have been used to image ablatively accelerated targets. Flash x radiography[12,13] is applied here to planar target geometry to extend the probing photon energy by about 10^3 beyond the visible, thereby gaining simultaneous access to the front and rear, as well as the dense middle, of accelerated, high velocity targets. The experimental setup is diagrammed in Fig. 1. A pinhole camera using photographic film recorded the image of an x-ray source, an aluminum plasma produced by a 20J, 0.6 nsec laser pulse.[11] The object to be radiographed was placed between the source and the pinhole; source x rays absorbed by the object result in a shadow image of the object on the film. The objects radiographed were planar foil targets of pyrolytic graphite having areal densities in the range of $1.0 - 1.5$ mg/cm^2. The backlighting x-ray flash was short enough that, for these targets, the travel distance during the flash (i.e., the velocity smearing) was comparable to the pinhole camera resolution (20 microns), thus enabling good image contrast to be achieved. The carbon (C) foils were accelerated by NRL's Pharos II laser operating at 1.05 microns with 3.3 nsec ($\pm 10\%$) driver pulses focused to 0.7-1.0 mm diameter. For some shots, a double foil target[10.4-5.8] was used, in which an impact foil, located behind the irradiated first foil (see Fig. 1), serves as a diagnostic of the motion of the first foil.

The source must be properly placed and timed to flash when the accelerated foil target moves into the view axis. A complication arises since the foil is also an x-ray emitter; therefore, we chose to radiograph the accelerated foil after it had ceased to emit, i.e., at a time 4-5 nsec after the peak of the main (driver) pulse. An x radiograph of a C foil irradiated at 6.5×10^{12} W/cm^2 is shown in Fig 2a. The backlighting source's emission is imaged on the left and the foil's emission is imaged on the right. Furthest to the right, x rays emitted by the C blowoff plasma are imaged. Since the C foil is wider than the laser's focus, only the central, irradiated portion of the foil is accelerated, leaving the rest of the foil behind. The shadow of this stationary margin may be seen in the image of the foil's own emission, i.e., as a self-radiograph (see Fig. 2a). Since the accelerated portion of the C foil moves several foil thicknesses while radiating, some of the self-emission occurs to the left of the stationary foil's shadow. After the driver laser pulse shuts off, the accelerated portion ceases to radiate but continues to fly to the rear (left). The flash x-ray source was positioned just to the left of the stationary foil's shadow, but extended several hundred microns further to the left than the self-emission. Within this several hundred microns, the shadow of the moving foil is clearly seen and appears connected to the stationary margin. Several interesting measurements can be made from this representative image.

SOURCE (Al SLAB)

SHORTENED LASER BEAM

OBJECT (C FOIL)

MAIN LASER BEAM

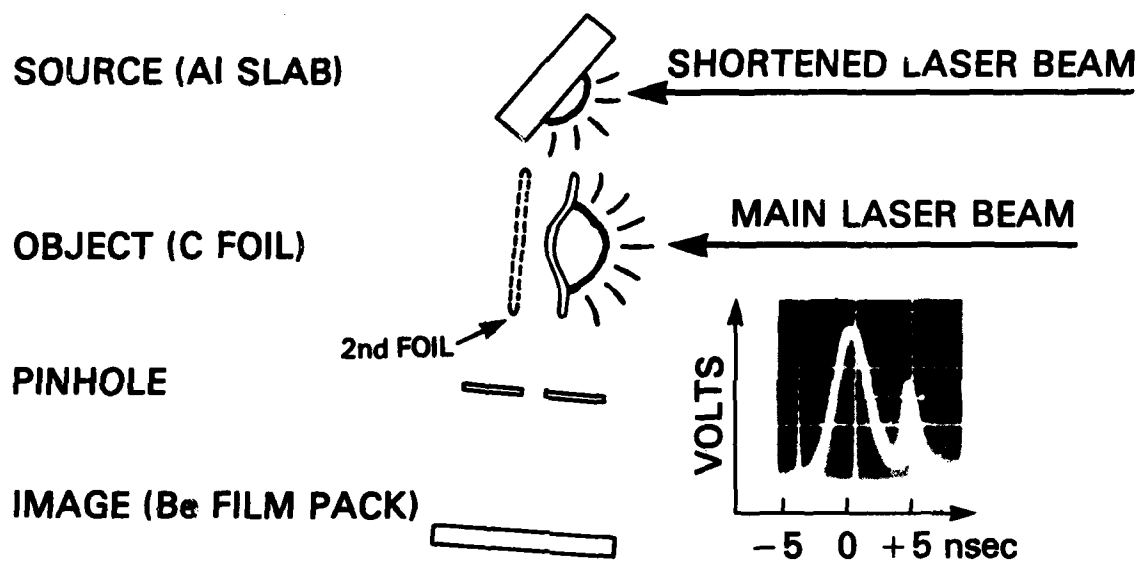2nd FOIL

PINHOLE

VOLTS

IMAGE (Be FILM PACK)

−5 0 +5 nsec

Fig. 1 — Setup for flash x-radiography (not to scale). Two 1.05 micron laser beams were focused through an f/6 lens onto separate targets. An absorption radiograph of the backlit object was recorded on x-ray film by a pinhole camera. Objects composed of single or double carbon foils were employed. Inset scope trace shows temporal shape of the main laser beam (peak at $t = 0$.) and delay of the backlighter's laser pulse (5 ns).

Using the stationary foil's shadow as a fiducial of the original position and taking the accelerated foil's shadow as the final position, an average velocity $v = s/\tau_d$ may be computed, with τ_d the delay of the x-ray flash. The result is 3×10^6 cm/s for this shot, for an energy density of 5×10^5 J/g on the axis of the driver laser. The energy in the accelerated foil was $E_t = (1/2)A\rho_a v^2$, where A is the area and ρ_a is the areal density. The initial 1.3 mg/cm^2 may be taken as ρ_a, since other measurements[4,5] indicate that less than 20% of the thickness would ablate by the time of observation. This leads to an estimate of total kinetic energy in the target of $E_t = (1/2)mv^2 = 1.5$J. The incident laser energy E_L was 76. J, from which the coupling efficiency, one of the critical elements,[2] was $\eta = E_t/E_L \times 100 = 2\%$; higher values are achieved when a larger fraction of the target is ablated.[3] This efficiency combines laser absorption and hydrodynamic acceleration processes.

Ablation pressure may also be obtained from these data, using $P = \rho_a v/\tau_L$, where τ_L is the FWHM of the main laser. This leads to a pressure estimate of 1.4 Mbar, at an incident irradiance of 6.5×10^{12} W/cm.^{2} This is in good agreement with pressures inferred from measurements on ablation plasma,[4] which showed a value of 1.7 ± 0.3 Mbar at an absorbed irradiance of 6.5×10^{12}. The pressure and velocities obtained using the double foil technique[5] are in similar agreement with the value obtained here.

However, our pressure results do not agree with the recently reported[14] 1.0 Mbar (at increased irradiance, 3.6×10^{13} W/cm^2) which was found to be 5-10x lower than cited measurements on ablation plasma.[14] In that work, a smaller spot size (200×300 μm^2), a shorter driver pulse (0.8 ns), and a longer probe pulse (0.8 ns) were employed. At our 3 nsec pulse length, lateral energy flow within the blowoff[8] extends as far as 140 microns at about 1×10^{13} W/cm^2; therefore, we have used focal spot diameters several times this length to avoid a reduction in pressure due to lateral flow of energy to regions outside the focal spot. Also the longer pulse lengths achieve a more predominately steady state ablative acceleration. However, the actual source of the discrepancy noted in Ref. 14 remains unresolved.

A further measurement of the image in Fig. 2 shows that the on-axis thickness of the shadow of the moving foil is about 35 - 70 microns. Pinhole resolution (20 microns), velocity smearing (about 20-30 microns), and geometric factors including parallax, foil rotation, and foil curvature, make the 70 microns an upper bound for the axial extent of this highly absorbing foil. It is estimated from the x-ray attenuation of un-ionized C that the observed absorption images (mostly 1.6 kev photons, taking a 1/4 mm photon path) represent, as a lower bound, a density of about 3% of solid. Shorter path lengths, higher photon energies, and increased ionization would raise this estimate. Since the x-ray range at 1.6 keV is only 8 microns, there were at most a few solid bodies, if any, of this size or larger outside the shadow region of the accelerated foil; the high density region was therefore localized to within the shadow.

The observation of a connecting structure of the shadow (Fig. 2a) strengthens the validity of both the double foil technique and the measurements of low preheat obtained for thin, planar targets.[6] One might intuitively expect that an accelerated disc would part from the unilluminated foil, leaving a break, through which plasma could flow and heat the rear of the foil. Double foil collisions would then be influenced by such spurious preheat. Previous investigation using optical[6] and double foil[5] techniques showed no evidence of such a plasma flow (see Fig. 1 in Ref. 6). The connecting structure observed in Fig. 2a evidently isolates the cool, rear surface from a hot plasma flow from the laser side. Thus, the x radiographs explain how low rear surface temperatures[6] of below 8 eV are maintained.

Looking at the finer details in Fig. 2a, there is an evident waviness to both front and rear sides of the accelerated foil's shadow. However, neither the source emission nor C foils, of the type used, have nonuniformities of the amplitude and wavelength needed to explain the waviness.[11] On the other hand, irradiance nonuniformities are known to exist and to influence target motion. The laser's focal spot distribution was taken on the same shot and shows illumination nonuniformities of about 3:1, with a spa-
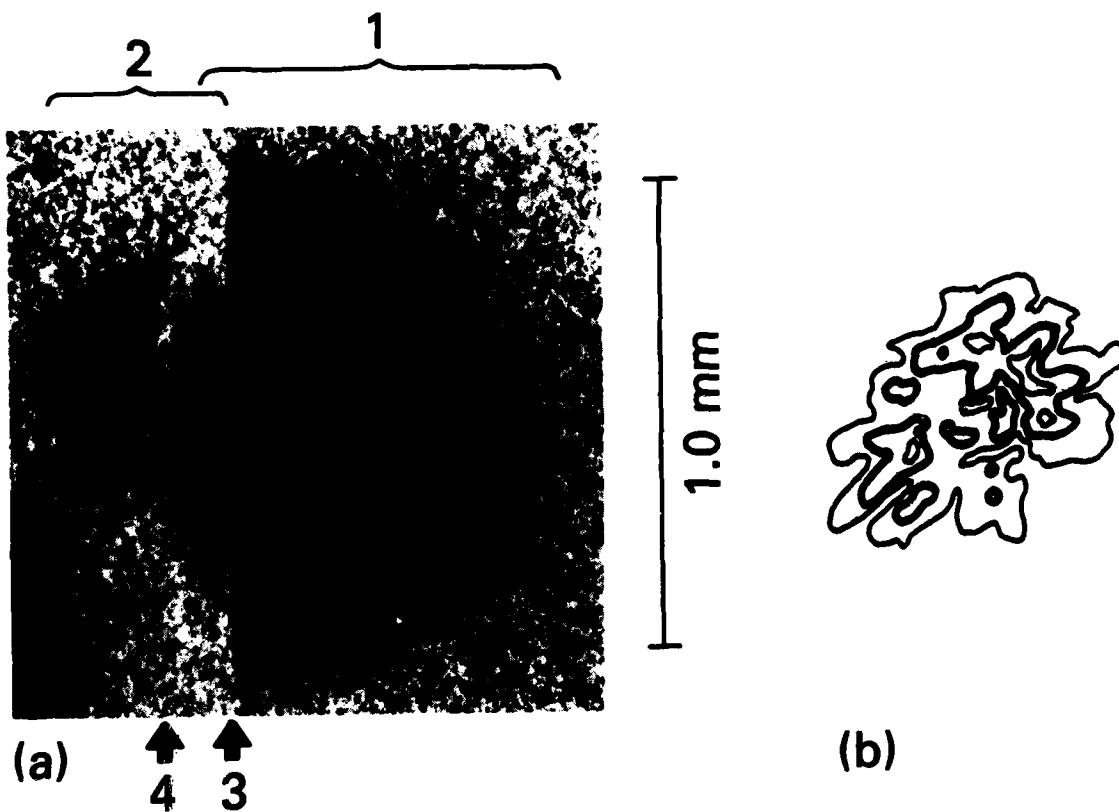
3

Fig. 2 — (a) Flash x radiograph of a single, 1.3 mg/cm^2 carbon foil moving at 3×10^6 cm/s: 1) C plasma emission; 2) Al source emission; 3) shadow of unaccelerated C foil; 4) shadow of accelerated C foil. (b) Intensity contour profile of the main laser beam's focal spot. The middle contour level is drawn in thicker lines for comparison with (a). Incident irradiance was 6.5×10^{12} W/cm^2, with 90% of the laser energy in a 0.7 mm diam. spot. The peaks of the two laser pulses were 4.9 ns apart. Shot 81-10636.

tial wavelength of about 75 to 100 microns. The waviness in Fig. 2a, which may be quantified as about 25% of the distance travelled, represents a lateral profile of nonuniformities in the target's velocity. The relationship between velocity nonuniformities and irradiance nonuniformities has been investigated previously and a smoothing of impressed laser nonuniformities has been observed in the target's motion.[7,8] Given the 3:1 nonuniformity in the laser, the amplitude of the waviness in Fig. 2a is consistent with the earlier measurements. Also, the spatial wavelengths of the waviness agree with those of the focal distribution (see Fig. 2b). Therefore, we conclude that the waviness in target motion is most probably a result of laser illumination nonuniformity. It is not necessary to invoke instabilities to explain this waviness.

Since smoothing enters into one of the critical elements, i.e., symmetrization, the smoothing was experimentally investigated by x radiography, using deliberately nonuniform illumination. A 2.0 cm opaque strip was placed across the entire diameter of the main laser beam and parallel to the backlighting viewing axis.[9] This produced a peak to valley ratio of about 6:1 in focused intensity on the C foil, and a valley width of about 140 microns.[8] The x radiograph in Fig. 3a clearly shows that a lower average velocity was reached in the valley of illumination. The peak and valley displacements, measured densitometrically from the moving foil's shadow, yield an average smoothing index $S = (V_{max}/V_{min}) - 1$, of $S = 0.4$ at an overall average incident irradiance of 3.6×10^{12} W/cm^2. This value is consistent with previously reported smoothing results (S slightly greater than 0.3), as determined with the double foil technique[8] for these conditions.

We briefly studied the double foil interaction by x radiography (see Fig. 1), both without and with a strip in the main laser beam. For this purpose, x radiographs are superior to previous diagnostic results using visible light, since the high density foils can now be seen in flight. Prior to impact, the first foil showed the connecting structure discussed above, while the accelerated region appeared more planar in one double foil image than did the foil in Fig. 2 for the same delay time. However, the overall indication is that the interaction of the two foils is not strongly governed by the low temperature plasma known to exist between them,[6,9] since the second foil remains in place, awaiting the impact. This conclusion is further strengthened by the x radiography of closely spaced double foils after impact, again using the 2.0 cm strip in the beam. The structure of the first foil was clearly registered on the impact foil, to the degree that the x-ray image appears almost identical to Fig. 3a. Thus, the impact of the high density regions of the two foils is the dominant interaction for double foils, under the conditions employed here.

In summary, flash x radiography has proven to be a valuable diagnostic for studies of the laser-target interaction and the acceleration of matter to high velocities. Measurements of, or observations relevant to, several important parameters have been made: coupling efficiency, symmetry (irradiance smoothing $S = 0.4$ at 4×10^{12} W/cm^2), velocity (30-50 km/s), pressure (1.4 Mbar at 6.5×10^{12} W/cm^2), and preheat (spurious heating prevented by the connecting structure). X radiography brings a significant improvement over visual probing techniques and has verified that we are accelerating high density material to high velocities.
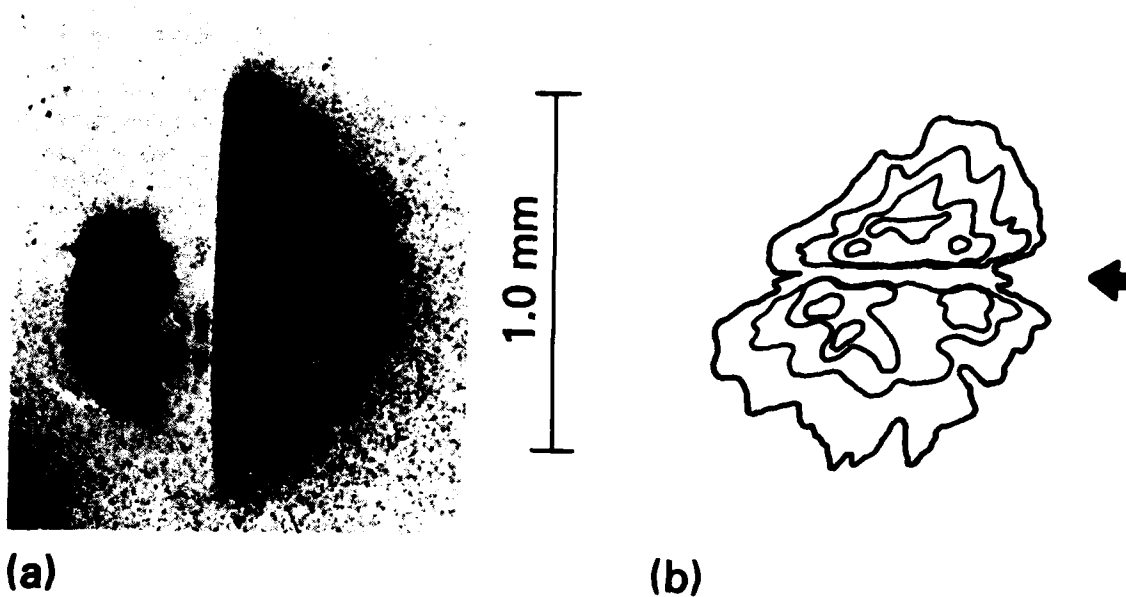
(a)

(b)

Fig. 3 — (a) Flash x-radiograph at 4.3 ns delay of a single, 1.5 mg/cm^2 foil with a nonuniform velocity profile produced by intentionally nonuniform illumination at 3.6×10^{12} W/cm^2. (b) Intensity contours of the 0.7 mm diam. focus, viewed perpendicular to (a). Arrow indicates valley in illumination profile produced by a 2.0 cm opaque strip which occluded part of the lens from the incoming laser beam. Shot 81-10676.

REFERENCES

1. J. Nuckolls, L. Wood, A. Thiessen, and G. Zimmerman, Nature *239*, 139 (1972).

2. S.E. Bodner, J. Fusion Energy *1/3*, pp. 221-240, (1981).

3. R. Decoste, S.E. Bodner, B.H. Ripin, E.A. McLean, S.P. Obenschain, and C.M. Armstrong, Phys. Rev. Lett., *42/25*, 1673-7 (1979).

4. J. Grun, R. Decoste, B.H. Ripin, and J. Gardner, Appl. Phys. Lett. *39/7*, 545-547 (1981); J. Grun, NRL-MR 4491 (May 8, 1981).

5. J. Grun, S.P. Obenschain, B.H. Ripin, R.R. Whitlock, E.A. McLean, J. Gardner, M.J. Herbst, and J.A. Stamper, NRL-MR 4747 (1982), submitted to Phys. Fluids.

6. E.A. McLean, S.H. Gold, J.A. Stamper, R.R. Whitlock, H.R. Griem, S.P. Obenschain, B.H. Ripin, S.E. Bodner, M.J. Herbst, S.J. Gitomer, and M.K. Matzen, Phys. Rev. Lett., *45/15*, 1246-1249 (1980).

7. S.P. Obenschain, R.H. Lehmberg, and B.H. Ripin, Appl. Phys. Lett. *37/10*, 903 (1980).

8. S.P. Obenschain, J. Grun, B.H. Ripin, and E.A. McLean, Phys. Rev. Lett., *46/21*, 1402 (1981) and *48/10*, 709 (1982).

9. B.H. Ripin, R. Decoste, S.P. Obenschain, S.E. Bodner, E.A. McLean, F.C. Young, R.R. Whitlock, C.M. Armstrong, J. Grun, J.A. Stamper, S.H. Gold, D.J. Nagel, R.H. Lehmberg, and J.M. McMahon, Phys. Fluids, *23/5*, 1012-1030 (1980); and Phys. Fluids *24/5*, 990 (1981).

10. B.H. Ripin, S.E. Bodner, S.H. Gold, R.H. Lehmberg, E.A. McLean, J.M. McMahon, S.P. Obenschain, J.A. Stamper, R.R. Whitlock, and F.C. Young, H.R. Griem, J. Grun, and M.J. Herbst, NRL-MR 4212 (16 May 1980).

11. R.R. Whitlock, S.P. Obenschain, J.Grun, J.M. McMahon, B.H. Ripin, and J.A. Sprague, article in Proceedings of the Topical Conference on the Symmetry Aspects of Inertial Fusion Implosions, S.E. Bodner, ed., (May 27-28, 1981, at NRL), to appear as an NRL report.

12. M.H. Key, C.L.S. Lewis, J.G. Lunney, A. Moore, T.A. Hall, and R.G. Evans, Phys. Rev. Lett., *41/21*, 1467 (1978).

13. H. Azechi, S. Oda, M. Hamano, T. Sasaki, T. Yamanaka, and C. Yamanaka, Appl. Phys. Lett. *37/11*, 998-1000 (1980).

14. A. Raven, H. Azechi, T. Yamanaka, and C. Yamanaka, Phys. Rev. Lett., *47/15*, 1049 (1981).

ATE
LMED
8